

DB

AN EXPERIMENTAL RECIPROCATING EXPANDER FOR CRYOCOOLER APPLICATION

Moses Minta and Joseph L. Smith, Jr.

Cryogenic Engineering Laboratory
Massachusetts Institute of Technology
Cambridge, MA 02139

An experimental reciprocating expander has been designed with features appropriate for cryocooler cycles. The expander has a displacer piston, simple valves, and a hydraulic/pneumatic stroking mechanism. The expander has a valve in head configuration with the valves extending out the bottom of the vacuum enclosure while the piston extends out the top. The expander has been tested using a CTI 1400 liquefier to supply gas at about 13 atm in the temperature range 4.2 to 12 K. Expander efficiency has been measured in the range 84 to 93% while operating the apparatus as a supercritical wet expander and in the range 91 to 93% as a single phase expander. The apparatus can also be modified to operate as a compressor for saturated helium vapor.

Key words: Cryogenic expander; two-phase expander; experimental expander; reciprocating expander; expander valve actuator; expander efficiency.

1. Introduction

Small cryogenic refrigerators have been extensively and successfully used to meet the low power refrigeration requirements of cryopumps, cryogenic sensors and electronic systems at temperatures above 20 K in the past decade. Most of these cryocoolers have been based on the Gifford-McMahon, Modified Solvay, Stirling, or Vuilleumier cycle. The modification required to meet low power refrigeration needs below 6 K result in considerable increase in cost, power and complexity. This makes cryocoolers based on work-extraction devices attractive, particularly because of increased efficiency.

Large capacity helium liquefiers invariably use the Collins two-expander cycle. These units use reciprocating expanders or turbo-expanders which appear unattractive for scaling down to low capacity helium liquefaction. In the case of turbo-expanders, this is because of an efficiency penalty since the losses scale down disproportionately with geometric size. By contrast, the principal losses associated with the reciprocating machine are heat transfer losses which may be minimized by proper design. These losses may be grouped, generally, into those affecting the power and those directly manifesting themselves as heat leaks to the working fluid.

The power losses are due to valve flow, leakage, mechanical friction, blow down, blow in, and cyclic heat transfer. The cyclic heat transfer loss is the result of periodic heating and cooling of the working gas by the cylinder walls. The incoming gas is warmer than the cylinder walls and is therefore cooled while the cold gas after the expansion process is warmed by the cylinder walls. The net effect is that the expander processes more gas without a corresponding increase in expander work per stroke. The heat input losses consist of static heat leak, shuttle heat transfer and cylinder-piston gap pumping loss.

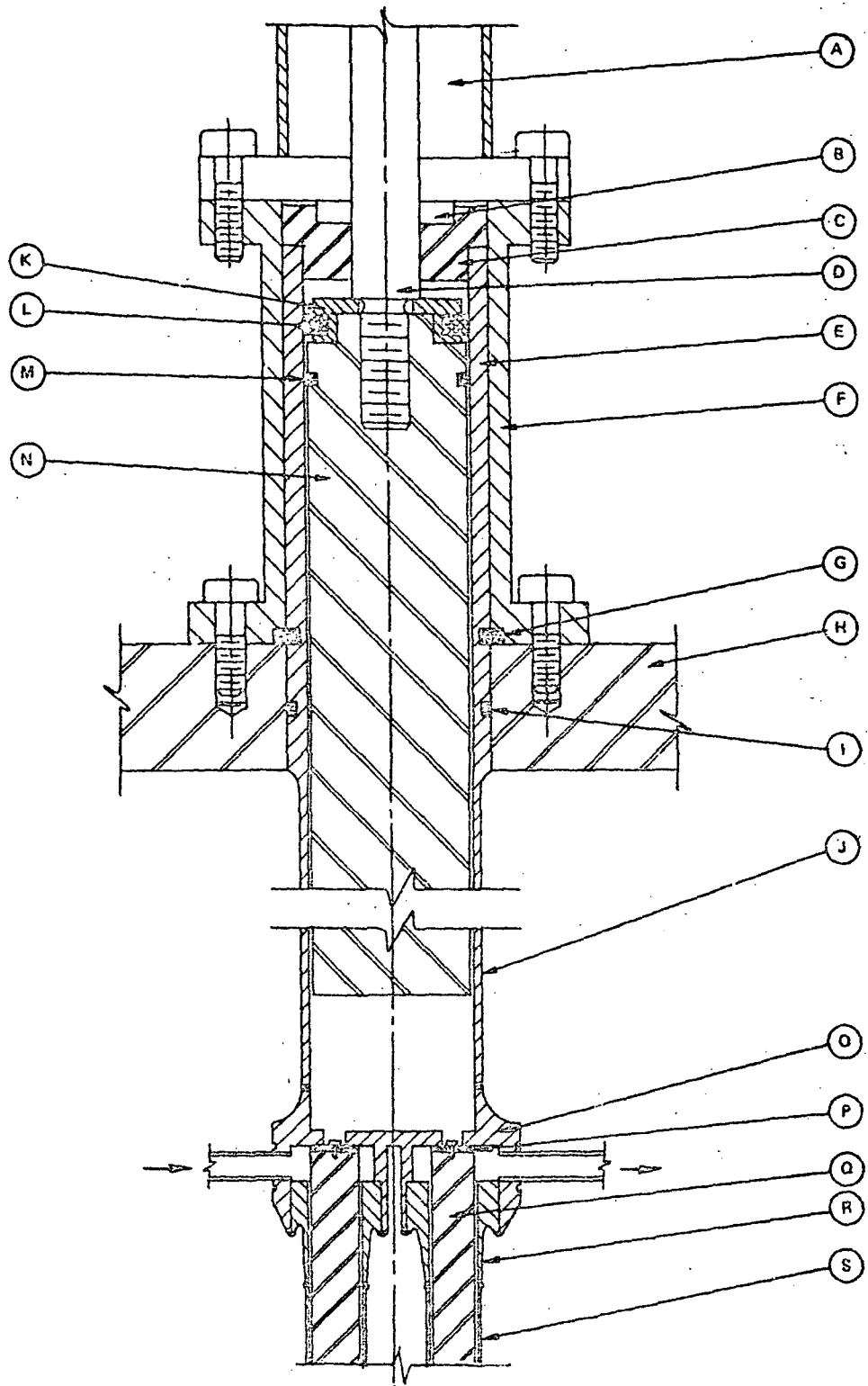


Figure 1. Cross section of expansion engine

Recent advances, especially in heat transfer analysis and experimentation have enhanced our understanding of the losses associated with the expander, and analytical models of varying sophistication and adequacy are now available for the losses¹⁻³. This has made it possible to design an efficient reciprocating expander. However, noise vibration and size considerations of the work-absorbing assembly associated with the conventional reciprocating expanders still limit the practicality of scaling down these units. This paper describes an experimental reciprocating expander⁴ which has been designed for high efficiency and uses a hydraulic-pneumatic drive mechanism and a pneumatic valve actuator in place of the flywheel, brake motor, mechanical cam-actuator assembly used in conventional large capacity liquefiers. The device can therefore be scaled down for cryocooler applications.

2. Description of expander

The reciprocating expansion engine, Fig. 1, consists of a long displacer closely fitted inside a long cylinder which hangs from a base plate, which is the top plate of a vacuum chamber. Above the base plate is an adjustable hydraulic-pneumatic system for piston motion and valve control. The valves for the engine extend down from the cylinder head. Surge chambers are located at the inlet and exhaust of the expansion engine to convert the pulsatile flow to a relatively smooth and continuous flow. Detailed description of these components follow.

The cylinder is made of 304 stainless steel because of its high strength to thermal conductivity ratio, low specific heat capacity and lack of brittleness at low temperatures. The thin wall of the cylinder coupled with low thermal conductivity of the material minimizes the conduction loss. Stiffening rings spaced 1.5 in apart around the outside diameter keep the tubing round. The thin wall tubing is TIG welded to the valve block (cylinder head containing the valve ports) at one end and a thick wall tube at the warm end used for mounting the engine. A solid phenolic micarta rod is used for the displacer because of its good wear characteristics. Also the thermal contraction characteristics closely match those of the stainless steel. The diametral clearance between the piston and cylinder is 0.005 in and is chosen by consideration of the shuttle heat transfer loss, the possibility of seizure due to small solid impurities and the possibility of displacer-cylinder contact.

The engine uses a single buna O-ring seal M at the warm end of the displacer-cylinder assembly. An oily felt washer L provides continuous lubrication for the O-ring. Thus there is minimal wear which reduces the possibility of wear material contamination. Also the small frictional heat generated is dumped into the atmosphere and does not detract from the cooling power of the engine.

Since the radial clearance on the 33-in-long displacer N is 0.003 in, only a small misalignment will cause the displacer-cylinder assembly to bind. The vertical alignment of the engine avoids gravity side loads and associated rubbing. The displacer is rigidly threaded to the piston rod D of a tandem cylinder assembly A. The tandem cylinder has four rod seals and two piston seals. Therefore the integral unit consisting of the tandem piston rod and the engine displacer ride on a total of seven supports of close tolerances. By proper initial positioning, the unit can be maintained reasonably well aligned in the vertical. The axes of the engine cylinder and the tandem cylinder are aligned by piece C, which fits inside the engine cylinder E and outside the bushing B at the end of the tandem cylinder. The cylinder is rigidly supported at the warm end on top plate H and extends into the vacuum chamber. The warm end of the cylinder E is attached to the plate by a split ring, groove and clamp flange, G and F.

Since throttling in the valves degrades the performance, the valve ports are located in the cylinder head to allow for reasonably large ports with minimum throttling. This port location also helps to reduce the clearance volume. The ports are 1/4-in holes drilled through the valve block/cylinder head O which is TIG welded to the cylinder J. Tubular valve sheaths S of 304 stainless steel are also welded to the valve block and extend from the bottom of the engine. These tubular sheaths enclose the valve pull-rods Q. The valve face, P, is a teflon disk mounted on the cold end of the phenolic micarta pull-rod with a screw and locked in place with a Belleville washer. The valve is held closed by the spring in the miniature air cylinder which actuates the valve. A buna O-ring serves as the warm end seal on the valve rod which fits closely in the sheath. Because of the rather short travel of the pull-rods, no lubricant reservoir is provided for the O-ring. The pull rod is adequately guided by the sheath since the clearance in the sheath is only 0.003 in.

3. Hydraulic-pneumatic piston-motion control system

The overall layout for the control system is shown in Fig. 2. Air limit switches send position signals to the air controller. The controller sends direction and speed signals to the control valves to control piston direction and speed. The hydraulic controller absorbs the expander work, and sets three different speeds during the exhaust stroke, the intake stroke and the expansion stroke. The expander work is dissipated in flow control valves in the hydraulic circuit.

The principal components of the hydraulic controller are three adjustable flow control valves G1, G2, G3 and a three-way hydraulic valve H (Fig. 2). The three-way valve is a two-position, single-air-piloted, spring-return valve. The oil flow through this valve is through valve G3 when there is air pressure at the pilot, or through line G4 when there is no air pressure. The adjustable flow control valve is a throttle and check valve combination which allows throttled flow in one direction and full flow in the other. Valves G2 and G3 restrict flow during the power stroke, while valve G1 restricts flow during the exhaust stroke. Therefore the setting on valve G1 determines the engine speed during the exhaust stroke. Valve G3 is by-passed during this stroke. During the intake stroke, air pressure at the three-way valve H switches the oil flow to valve G3 which meters the flow together with valve G2. The valve settings on these two valves therefore determine the piston speed during the intake process. At cut off, air pressure is released on the three-way valve and the spring returns the oil flow to line G4. Valve G2 is now by-passed. There is full flow in valve G1 and metered flow in valve G2 which sets the piston speed during the expansion process. A bleed line L is provided for the hydraulic circuit. Also an air-pressurized oil reservoir is provided to maintain the oil under pressure and eliminate air leaks into the hydraulic circuit. With air in the oil the piston velocity cannot be controlled.

The heart of the air limit switch system is a miniature double-plunger two-position fully ported four-way spool valve F, Fig. 2. The valve is supported by threaded rods attached to the tandem-cylinder assembly. A yoke, BB, F1, and F2 is attached to the free end of the piston rod. At maximum volume, surface F1 actuates the plunger and at minimum volume surface F2 actuates the plunger of the spool valve. The stroke of the machine is adjusted by adjusting the vertical position of the four-way valve and the distance between F1 and F2. Threaded rods and nuts facilitate these adjustments.

The cut-off switch E sends a position signal to the pneumatic control at the end of the intake process. Switch E is a heavy duty miniature air limit switch. It is a two-position, plunger-actuated normally-closed valve. A cam, E1, attached to the piston rod actuates the cut-off switch. The output signal from switch E1 is used to actuate the expander inlet valve and the three-way hydraulic valve in the hydraulic controller. The cut-off switch is attached to the tandem cylinder with threaded rods for position adjustment. The expander cut-off point is adjusted by changing the position of this switch.

The two principal components of the pneumatic controller are a directional valve C and a NOT element B, which is described in the next paragraph. The directional valve is a heavy-duty, two-position, double-air-piloted, fully-ported, four-way spool valve. The pilot signals to operate the valve are supplied by the limit switches. The four way directional valve switches pressure and exhaust to the double acting pneumatic cylinder, thus providing pneumatic power for both the up (expansion) and down (exhaust) strokes. Thus the pneumatic driver can drive the piston even when no helium is being processed by the expander. This feature allows a later adaptation of the expander as a compressor.

The purpose of the NOT element is to provide the signals to open the engine inlet valve only at the end of the exhaust stroke, after the exhaust valve has been closed and to close the inlet valve at the cut-off point of the power stroke. The two input signals to this element are a signal from the cut-off switch to input port 1 and another signal from the end-of-stroke limit switch F to input port 2. The output of the NOT element is pressure at port 3 if there is pressure at input 1 and if there is no pressure at input 2. During the intake stroke the switch E is depressed sending pressure to port 1 of the not element B. There is no pressure at port 2 of B so pressure at 1 passes to 3. This pressure holds the inlet valve open and switches valve H causing hydraulic valve G3 to be active. At cut off, E switches which exhausts the pressure at 1. With no pressure at 1, the NOT element switches which exhausts the pressure at 3, closes the inlet valve, and allows valve H to spring return. At the end of the expansion stroke, valve F switches sending no pressure to E and pressure to port 2 which also opens the discharge valve. Switch E has no pressure and no influence as it is depressed during the discharge stroke. At the end of the discharge stroke valve, F switches pressure through E to port 1. Only after the pressure in the discharge valve actuator has dropped, does the NOT element B see no pressure at 2 and switch pressure from 1 to 3 which opens the inlet valve.

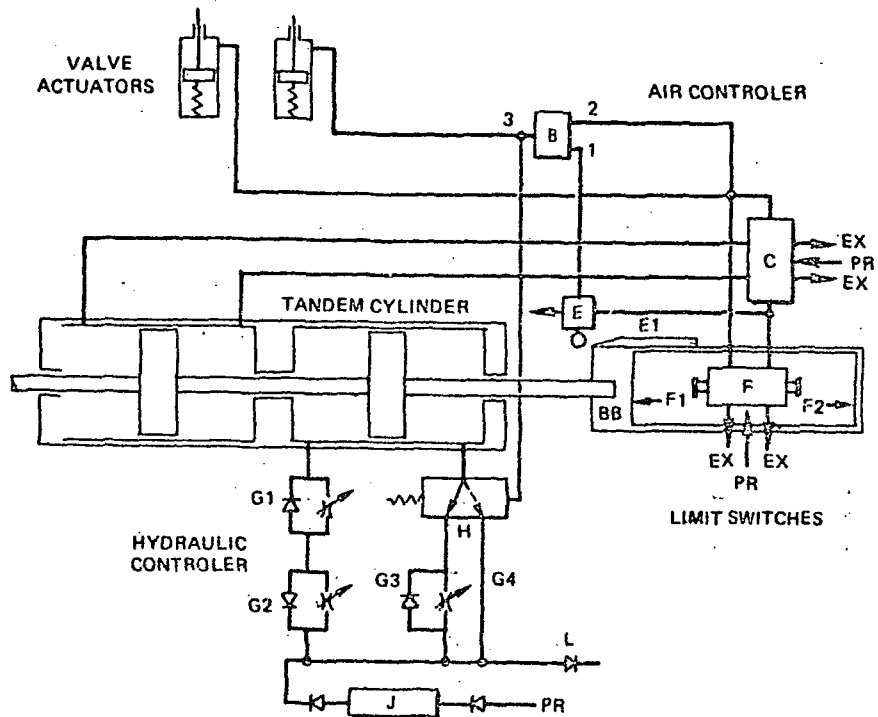


Figure 2. Hydraulic-pneumatic control system

4. Debugging the pneumatic circuit

The hydraulic and pneumatic system was assembled from standard catalogue item components. Since these were not optimum components and their internal design and port sizes were not readily available, an experimental rather than an analytical approach was used to tune and adjust the system. The pneumatic circuit was instrumented with several pressure transducers. The engine was instrumented for cylinder pressure and piston position. Data from these instruments were observed and recorded with a digital oscilloscope and subsequently transferred to a VAX computer for analysis. This data was sufficient to tune the system for satisfactory operation. Typical curves showing the phase relationships are shown in Fig. 3.

5. Time sequence in the expander

Fig. 3 shows piston position, inlet valve actuator pressure, exhaust actuator pressure, and expander cylinder pressure on the same time base for a typical cycle. Starting at TDC (minimum volume) with the inlet pressurized (open) and the exhaust closed (depressurized), the piston moves up at low velocity until the cutoff point (CO) is reached. The inlet valve closes and the hydraulic three-way valve switches to a low flow resistance (G4 of Fig. 2). The cylinder pressure falls rapidly and the piston velocity increases. When the piston reaches BDC (maximum volume) the exhaust pressurizes (opens) and the piston reverses direction. The piston moves rapidly to TDC (minimum volume). Subsequently the piston switches direction, the exhaust depressurizes (closes), and the three-way hydraulic valve switches to high flow resistance G3. The inlet then pressurizes (opens), to repeat the cycle. The cut off switch resets on the exhaust stroke, but has no action since it has no pressure supply.

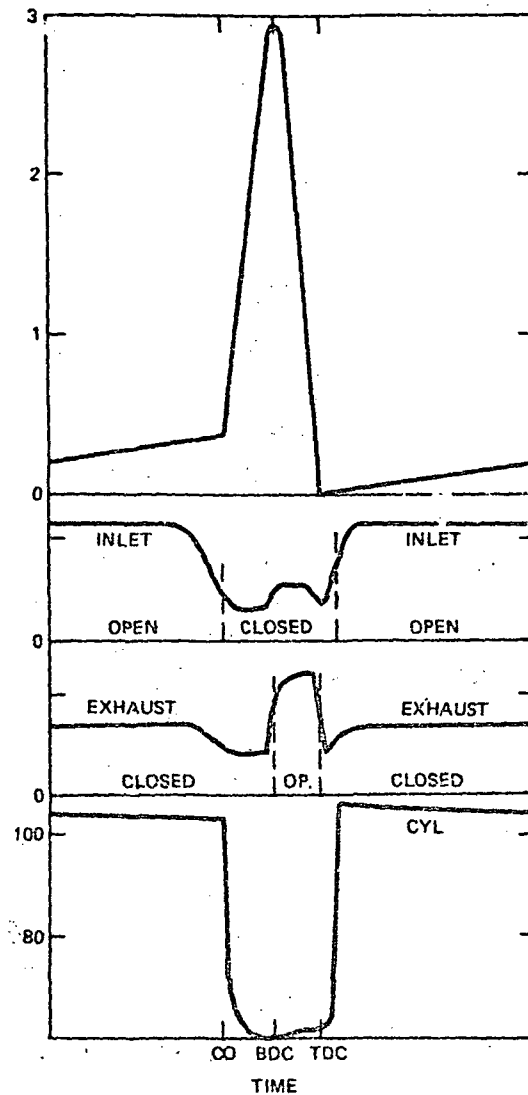


Figure 3. Expander cycle

Fig. 3 also shows that the times required to pressurize and depressurize the valve actuators are significant. The inlet valve actuator takes about 0.14 s to 0.16 s to pressurize up to full pressure (80 psig). However it takes about 0.06 to 0.085 s to reach the level high enough to switch the valve. On the other hand, depressurization takes about 0.20 to 0.24 s. Again the valve closes after about 0.16 s. Similarly, pressurization of the exhaust valve actuator takes between 0.10 and 0.12 s and depressurization about 0.14 s. The quicker response of the exhaust actuator results from its being connected directly to the limit switch whereas the inlet actuator is connected to the limit switch through a NOT element with a smaller port size than the air limit switch (Fig. 2). There is always a residual pressure at one of the actuators whenever there is pressure in the other. The residual pressure is about 6 psig for the inlet valve actuator and 12 psig at the exhaust valve actuator. There is no pressure in either actuator only during the expansion process (and also briefly at the end of the exhaust stroke before the inlet valve opens). There is also evidence of pressure signals propagating between components through the air pressure source because of the source impedance.

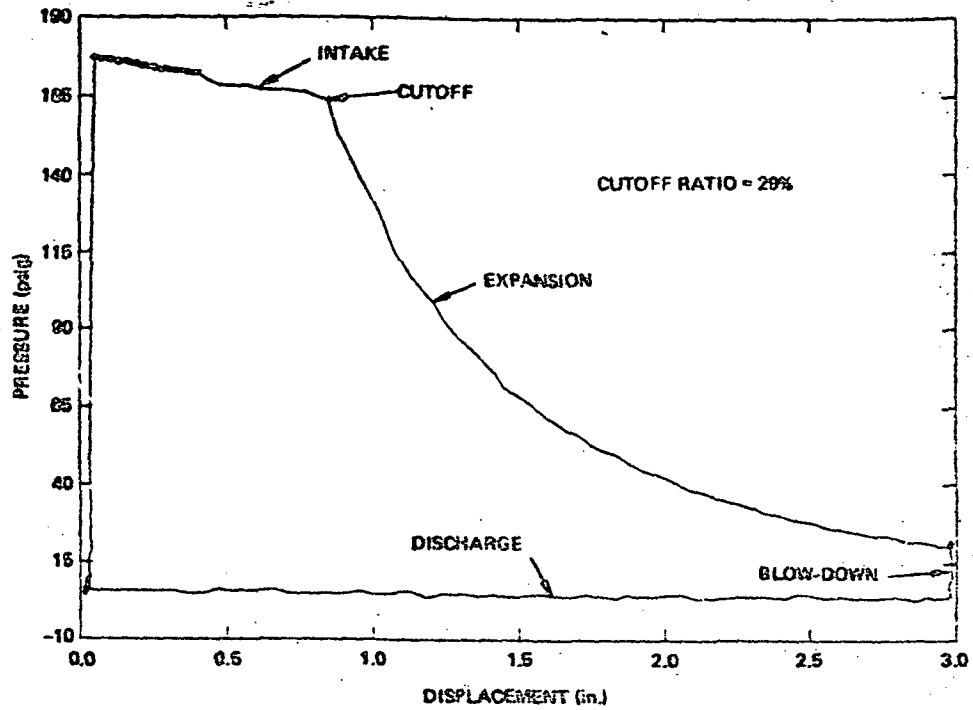


Figure 4. Pressure-displacement diagram for single-phase operation

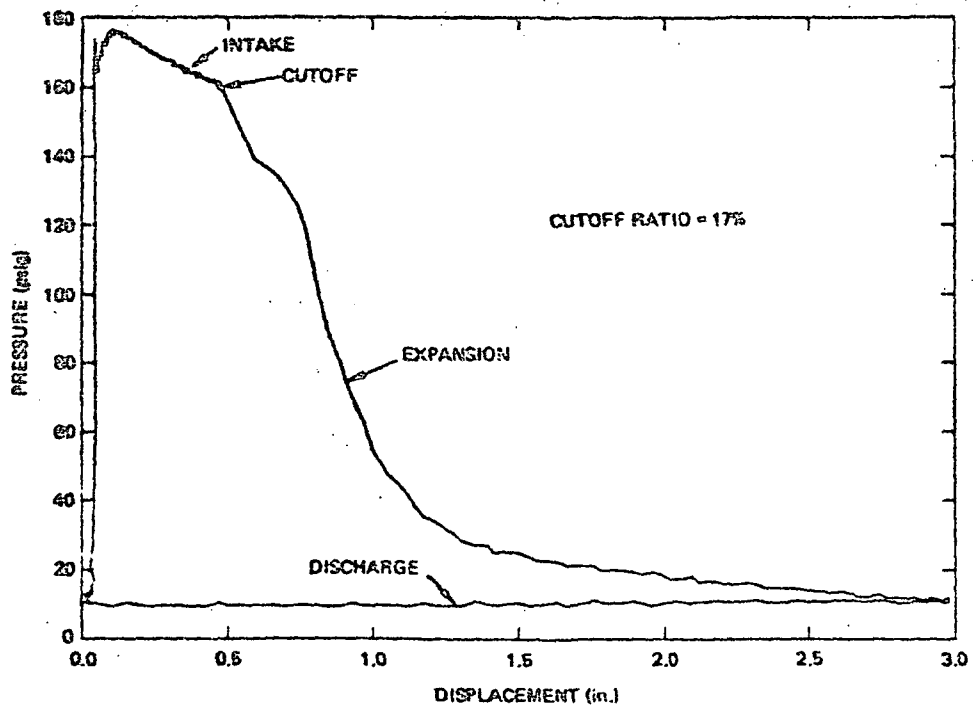


Figure 5. Pressure-displacement diagram for single-phase operation

6. Expander diagrams

Figures 4, 5, and 6 show typical pressure-displacement diagrams for the expander. The diagrams show a significant drop in pressure during the intake process. A surge chamber of approximately ten times the expander displacement was provided at the inlet and the piston speed during intake was kept minimal. The cause of the pressure drop in spite of these precautions is the high flow resistance in the J-I stage of the Model 1400 liquefier that supplied the inlet gas. A fairly constant inlet pressure was obtained in Fig. 4 for operation in the single phase region with a slow intake process. Table I summarizes time and speed distribution for a typical cycle.

Table 1. Typical time distribution for expander cycle

process	piston speed (in/s)	time (s)
intake	0.21	1.87
expansion	9.14	0.28
exhaust	7.76	0.38
dwell at TDC	-	0.10
dwell at BDC	-	0.04
total		2.76

The cycle of Fig. 4 has a blow down loss, while, in contrast, the cycle in Fig. 5 shows complete expansion. It was possible to adjust the cut-off point to ensure negligible blow down loss at the expense of expander capacity. The two cycles just described in Figs. 4 and 5 were obtained for single phase operation of the expander. The cut-off ratio is about 20%, which is defined as cylinder volume at the closing of the inlet valve divided by the maximum cylinder volume at the end of the stroke. The diagram of Fig. 6 was obtained for a comparable cut-off ratio and for operation in a two-phase expander mode. The diagram indicates an overexpansion followed by a small recompression.

7. Evaluation of engine performance

The reciprocating expander was tested as a supercritical wet expander and as a single phase expander using a CFI model 1400 liquefier to supply gas at about 13 atm in the temperature range of 4.2 to 12 K. The efficiency of the wet expander is defined with reference to Fig. 7 as

$$\text{efficiency} = \frac{W_{\text{act}}}{W_{\text{rev}}} \quad (1)$$

where

$$\text{actual work} = W_{\text{act}} = m(h_1 - h_3) + Q_{\text{act}}$$

$$\text{reversible work} = W_{\text{rev}} = m(h_1 - h_3) + Q_{\text{rev}}$$

$$\text{mass flow rate} = m$$

$$\text{actual refrigeration} = Q_{\text{act}}$$

$$\text{reversible heat input} = Q_{\text{rev}} = m T_{\text{sat}} (s_3 - s_1)$$

$$\text{inlet enthalpy} = h_1$$

$$\text{saturated vapor enthalpy} = h_3$$

The actual work is also given by the difference between the indicated work and the heat leak. This gives an alternative method for evaluating the efficiency. The measurements required to evaluate the performance are therefore: 1. The state (temperature and pressure) of the working fluid at the inlet and at the exhaust. 2. The actual refrigeration effect. 3. The indicated work from a P-V trace. 4. Heat leak by static conduction 5. Heat leak due to piston motion.

The experimental setup for obtaining these measurements is shown in Fig. 8. The states of the helium were measured in the inlet and in the heater tanks. The pressure was measured with a ugm pressure gage connected with capillary tubing. The temperature was measured using helium vapor pressure thermometers.

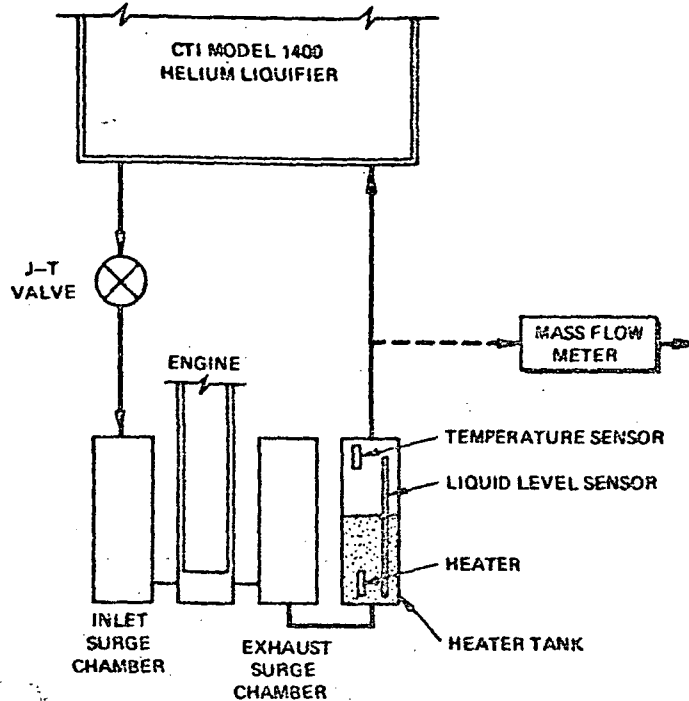


Figure 8. Expander test setup

Actual refrigeration capacity was measured as the power to the heating element. The heater power supplied was adjusted to be just sufficient to evaporate the liquid resulting from the expansion process so that the leaving stream was saturated vapor. The helium vapor pressure thermometer was provided to monitor that the gas was not overheated. It was also found necessary to use a liquid level gauge to maintain a steady liquid level in the heater tank.

The indicated work was calculated from measurements of the pressure inside the expander working space and the piston position. The pressure was measured using a high-impedance piezoelectric miniature pressure transducer operating at expander temperature. The charge output of the sensing element, a quartz crystal, was fed to a signal conditioning module and converted into a proportional voltage signal. The transducer was threaded into a mounting adaptor which was connected to the cylinder through a short capillary tube.

The static heat leak to the expander was measured with the engine valves propped open. The expander and the peripheral apparatus were then cooled down to the operating temperature by operating the liquefier on the J-T valve. The two-phase flow from the J-T valve was gradually reduced until a small temperature rise was detected across the expander. The temperatures were recorded from vapor pressure thermometers. To measure the mass flow rate, the cold return gas from the engine was warmed up external to the liquefier and then passed through a calibrated mass flow transducer.

Piston motion heat transfer loss was measured with the setup shown schematically in Fig. 8. The engine was first cooled down to the operating temperature. Both valves were propped open and the refrigeration capacity of the liquefier operating with the J-T valve was determined by measurement of heater power required to achieve saturated vapor at the heater tank discharge. With the valves still propped open, the piston was shuttled by means of the piston motion control system. Because of the heat loss through this piston motion, the heater supply power to boil away the liquid (indicating the refrigeration capacity) was reduced. The difference between the two measured capacities gave the loss due to the piston motion.

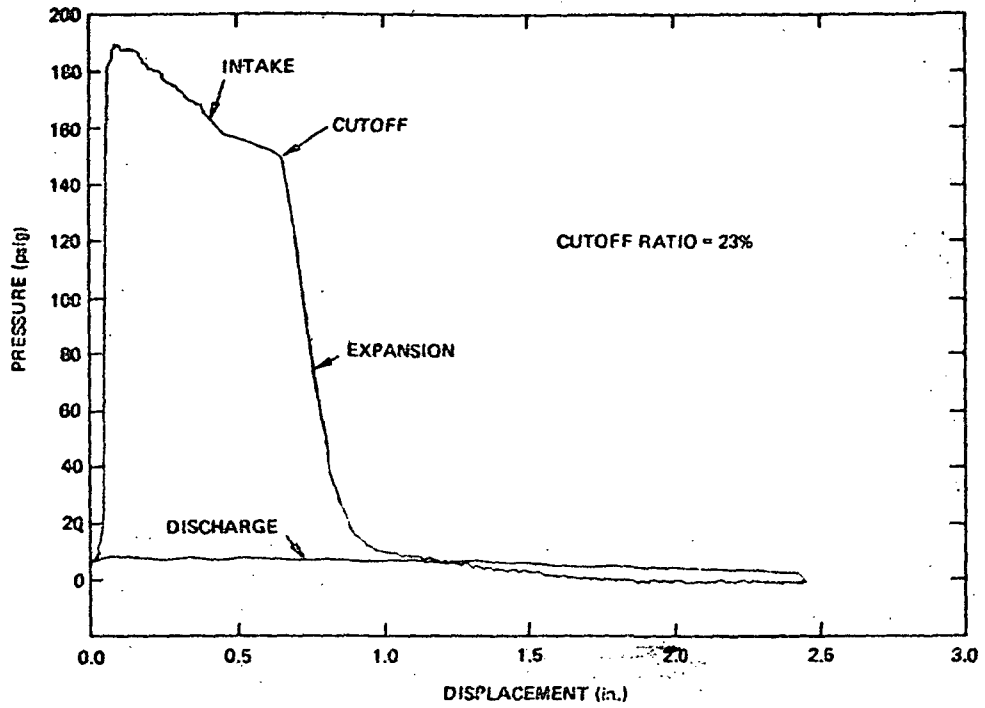


Figure 6. Pressure-displacement diagram for two-phase operation

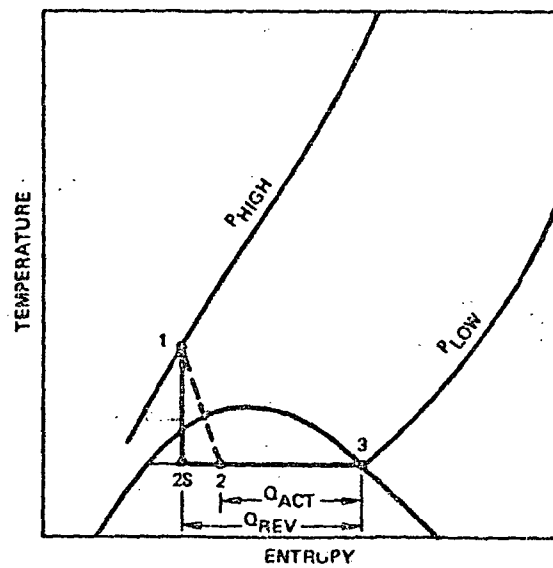


Figure 7. I-S diagram for two-phase expander

8. Results

Typical state point measurements are summarized in Table II. For the data of the Table, the single phase expander efficiency is 93 percent. For other tests the single phase expander efficiency ranged between 91 and 93 percent.

Table 2. Expander performance data

	single phase operation	two phase operation
Inlet pressure (atm)	13.21	13.24
Inlet temperature (K)	11.51	6.55
exhaust pressure (atm)	1.2	1.2
exhaust temperature (K)	4.72	4.42

The performance of the expander operating in the two-phase region was evaluated. Typical data are:

$$\text{Refrigeration effect} = Q_{\text{act}} = 33.4 \text{ W}$$

$$\text{Mass flow rate} = m = 2.18 \text{ g/s}$$

(from displacement and inlet state)

$$\text{Reversible work} = W_{\text{rev}} = 21.8 \text{ W}$$

$$\text{Actual work} = W_{\text{act}} = 20.4 \text{ W}$$

$$\text{Expander efficiency} = 94\%$$

The wet expander efficiency was also calculated from the indicated work and the measured heat leak losses. Typical data are:

$$\text{Indicated work} = W_{\text{ind}} = 21.4 \text{ W}$$

$$\text{Piston motion loss} = 1.3 \text{ W}$$

$$\text{Static heat conduction loss} = 1.6 \text{ W}$$

$$\text{Actual work} = W_{\text{act}} = 18.5 \text{ W}$$

$$\text{Expander efficiency} = 84.5\%$$

The two methods always gave values which differed by less than 10 percent. A major source of inaccuracy in the result is calculating the mass flow rate from the expander inlet temperature

9. Conclusion

The hydraulic-pneumatic mechanism for piston motion and valve control enabled fairly good control over the cycle events in the expansion engine. The high efficiencies measured demonstrate the potential for scaling down reciprocating expanders for cryocooler applications.

The expander was run only long enough to obtain performance data. No endurance data was taken because the system was assembled from inexpensive catalogue items which were not designed for long life. Most of the experimental difficulties were the result of the compromises required to use standard items for the hydraulic-pneumatic control system.

The research plan is to modify the apparatus for testing as a vapor compressor operating at 4.2 K. This test will require modification of the connections to the helium liquefier and a modification of the valve control sequence. These modifications are rather simple since the apparatus was designed for the compressor tests. If the compressor tests are as successful as the expander tests, the plan is to demonstrate the full potential of the saturated vapor helium liquefaction cycle. This will require the design an expander and compressor module to match the model 1400 liquefier, and the replacement of the J-T heat exchanger in the liquefier.

10. References

- [1] Rios, P. A., An approximate Solution to the Shuttle Heat Transfer Losses in a Reciprocating Machine, Journal of Engineering for Power, (April 1971).
- [2] Radebaugh, R. and Zimmerman, J. E., Shuttle Heat Transfer in Plastic Displacers at Low Speeds, NBS Special Publication 508.
- [3] Lee, K., Smith, J. L. Jr., and Faulkner, H. B., Performance Loss due to Transient Heat Transfer in the Cylinders of Stirling Engines, 15th Intersociety Energy Conversion Engineering Conference Proceedings, Vol 2, (1980).
- [4] Hintz, H., Analytical and Experimental Studies of a Helium Liquefaction Cycle, ScD Thesis, Department of Mechanical Engineering, MIT, (Feb. 1954).